Available online at www.sciencedirect.com
SCIENCE DIRECT®
ELSEVIER
Engineering Geology 68 (2003) 53–66
ENGINEERING GEOLOGY
www.elsevier.com/locate/enggeo

Nine years of spatial and temporal evolution of the La Valette landslide observed by SAR interferometry

C. Squarzoni[a,b], C. Delacourt[a,*], P. Allemand[a]

[a] *Laboratoire Sciences de la Terre, UMR 5570, Université Claude Bernard Lyon-1 et ENS Lyon, Bat Géode, 2 Rue Raphaël Dubois, 69622 Villeurbanne Cedex, France*
[b] *Dip. di Geologia, Univ. di Padova, via Giotto, 1-35137 Padova, Italy*

Received 2 October 2001; received in revised form 29 April 2002; accepted 24 May 2002

Abstract

The La Valette landslide located in the Ubaye valley (southern French Alps) has been investigated using 15 differential interferograms realized from ERS-1 and ERS-2 satellite radar images acquired between 1991 and 1999, both in 3-day cycle and TANDEM phase. Displacement values of the landslide have been deduced from the Synthetic Apenture Radan (SAR) interferometric products interpretation and compared with ground laser measurements. Four domains characterized by different velocity fields have been detected. Three of them can be distinguished from aerial photographs and field analysis. The slow velocity of a resistant bar located in the eastern side of the landslide has been detected on SAR interferograms. Between 1991 and 1996, changes in the landslide limits have been observed both in the upper and in the lower part; the changes have been caused by a retrogression of the main scarp and a down slope progression of the main body of the landslide, respectively. The average daily velocity of the landslide between 1991 and 1999 derived by interferometric analysis decreased from 1 to 0.4 cm/day, in agreement with ground-based measurements. A peak velocity of around 2 cm/day was observed in 1996.

Keywords: SAR interferometry; Landslide; Ground surface motion

1. Introduction

The study of the spatial and temporal evolution of the surface motion can help in the understanding the influence of the parameters controlling slow landslides (some centimetres per week over several years). A multiyear trend of velocity variation may be superposed on seasonal meteorological variation, and on episodic events. A multitemporal and multiscale study is required to decipher the signature of different causes. Kinematic studies are usually realized by techniques measuring punctual displacements (levelling, laser-meter, GPS), which may not be very suitable to reveal spatial heterogeneities of mass movements. Remote sensing techniques can help in landslide studies. In particular, SAR interferometry is a powerful tool, providing an image representing the motion with a centimetric precision and with a decametric resolution (Massonet et al., 1993). This technique has already proven its capability to detect and to map surface displacements caused by different natural and anthropic phenomena such as earthquake (Massonet et al., 1993;

* Corresponding author. Tel.: +33-472-44-84-13; fax: +33-472-44-85-93.
E-mail address: delac@alto.univ-lyon1.fr (C. Delacourt).

0013-7952/02/$ - see front matter © 2002 Elsevier Science B.V. All rights reserved.
PII: S0013-7952(02)00198-9

Zebker et al., 1994), ice sheet motion (Goldstein et al., 1993), volcanic activity (Massonet et al., 1995), land subsidence (Carnec et al., 1996; Fruneau et al., 1999). Despite some severe limitations (high vegetation density leading to decorrelation, high variation of topography, high deformation rate leading to loss of coherence, (Vanderbecq, 2000)), the capability of SAR interferometry to detect movement fields in landslide areas has been demonstrated (Fruneau et al., 1996; Carnec et al., 1996; Rott et al., 1999; Vietmeier et al., 1999).

In the present work, a landslide called La Valette, located in the southern French Alps is studied. This site has already been investigated with the same technique by Vietmeier et al. (1999). The data set processed by Vietmeier et al. (1999) consisted in three TANDEM pairs acquired from August 1995 to March 1996 using the technique of three-pass interferometry without Digital Elevation Model (DEM) elimination. The objectives of the work were the demonstration of the general capability of differential SAR interferometry to determinate the motion field of a landslide and to investigate the accuracy of the method. The present work is based on the study of 15 differential interferograms produced from SAR images acquired by ERS 1 and ERS 2 satellites between 1991 and 1999 (three of them are the same of Vietmeier et al., 1999) and proposes a multitemporal and spatial study of the landslide motion over 9 years. In the following, the La Valette landslide is described, the landslide area is analysed by means of ground survey and aerial photograph interpretation. Then, the interferometric data set is presented and the differential SAR interferograms are analysed and related to the local geological setting of the landslide.

2. Geological setting

The La Valette landslide is located in the southern French Alps, north of the Mercantour massif. The slope involved in the landslide movement is placed near the village of Barcelonnette, on the right side of the Ubaye valley, in the catchment of the La Valette stream (Fig. 1a). The geological setting of the surrounding zone is that of the Barcelonnette window structure, denudated by the Würmian Ubaye glacier. The base of the local geological succession, outcropping on the lower part of the landslide slope, is formed by the Callovo–Oxfordian "Terres Noires" formation, about 300 m thick and mainly composed of closely stratified black marls (Kerckhove, 1969). This formation is very sensible to physical weathering processes and erosion, locally causing voluminous solid transport and promoting surface instabilities (Antoine et al., 1995). The Helminthoid Flysch nappes, called Ubaye–Embrunais nappes and composed by Senonian sediments, tectonically overlie the "Terres Noires" formation (Fig. 1b). From the base to the top, the nappe pile is formed by (1) limestone scales of the Pelat nappe, called "Rocher Blanc", belonging to the Subbriançonnais units and dated Upper Cretaceous–Upper Eocene; (2) the Autapie nappe, mainly composed by black schists, locally with layers or blocks of limestone and sandstone; (3) the Parpaillon nappe made of flysch, forming the Soleil Bœuf ridge (Kerchkove et al., 1978) (Fig. 1b). The thrust puts in contact rocks with very different hydrogeological properties. Below the contact, the marls of the "Terres Noires" constitute an impermeable base. Over the contact, highly fracturated flysch formations are characterized by high permeability, which favours water circulation. Consequently, in correspondence to the thrust, a large number of springs has been mapped (Dupont and Taluy, 2000). On the lower part of the slope, up to 1500 m of altitude, a layer of clayey Würmian moraines covers the "Terres Noires" (Fig. 1b).

3. History of the La Valette landslide

The La Valette landslide started in 1982 with a deep fracture which opened just at the contact between the

Fig. 1. (a) Geological scheme of the Barcelonnette area (from Kerckhove, 1969, modified). (1) External crystalline massifs. (2) External zones (autochthon, from Trias to Priabonian; "Terres Noires" Formation in the Barcelonnette zone). (3) Subbriançonnais units. (4) Briançonnais zone: a, Permo-Carboniferous and Mesozoic units; b, Nummulitic Flysch. (5) Basal scale of Parpaillon nappe. (6) Autapie nappe. (7) Parpaillon nappe: a, basal schistose complex; b, Helminthoides Flysch and Embrunais Sandstone. The black lines represent structural elements. The black area north of Barcelonnette represents the La Valette landslide. A–A' represents the line of the cross section in b. (b) Geological cross section of the landslide: (1) Autochthonous: Callovo–Oxfordian "Terres Noires"; (2) Autapie nappe with a tectonic scale of limestone at the base (Rocher Blanc); (3) Basal scale of the Parpaillon nappe; (4) Parpaillon nappe, M–moraines. The landslide is shown in gray.

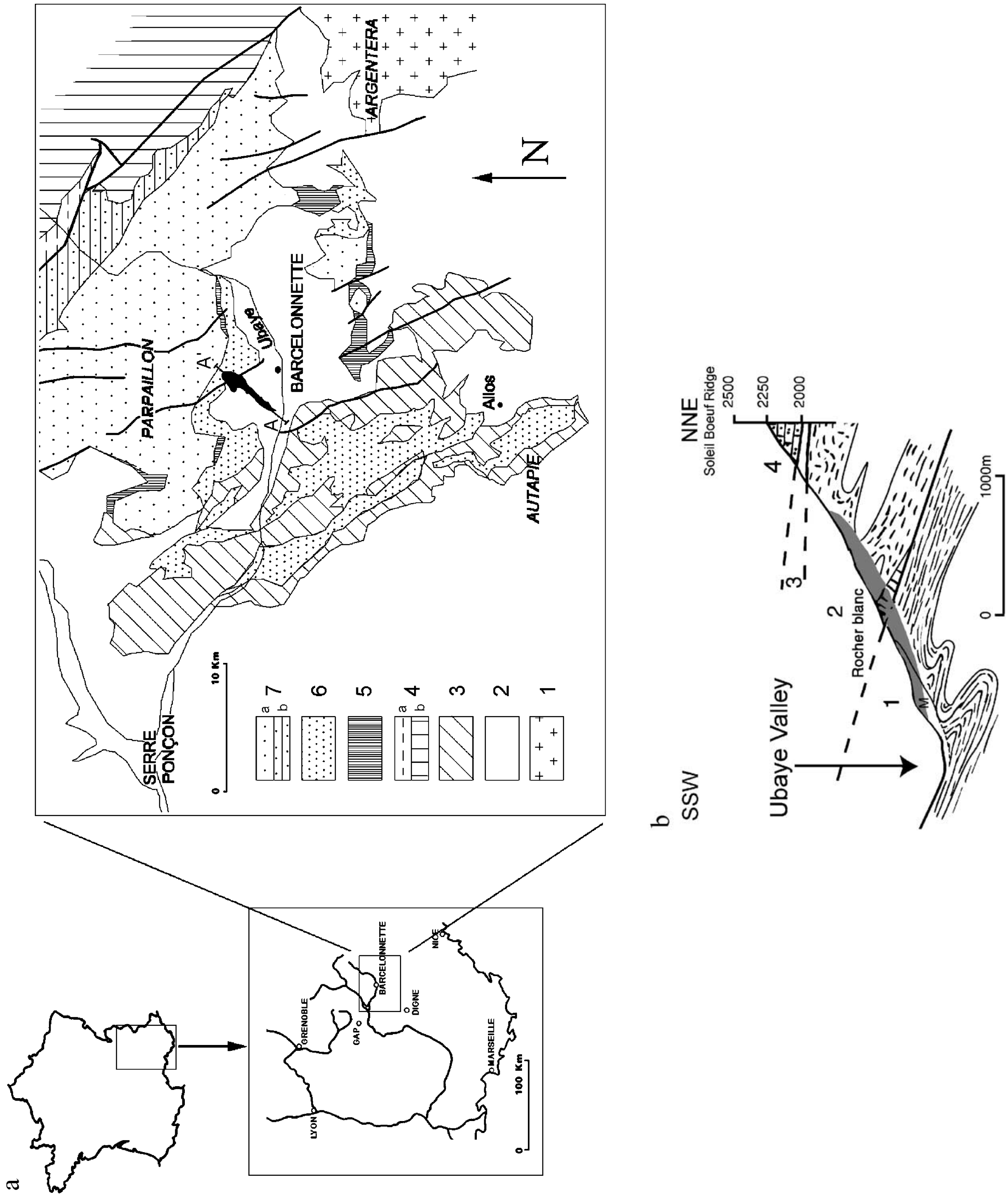
a
b
SERRE
PONÇON
PARPAILLON
BARCELONNETTE
ARGENTERA
AUTAPIE
Allos
Ubaye
A
A'
N
0
10 Km
7
a
b
6
5
4
a
b
3
2
1
GRENOBLE
BARCELONNETTE
NICE
GAP
DIGNE
LYON
MARSEILLE
0
100 Km
SSW
NNE
Soleil Boeuf Ridge
2500
2250
2000
Ubaye Valley
Rochet blanc
1
2
3
4
M
0
1000m

"Terres Noires" and the flysch nappes (Colat and Locat, 1993). The landslide developed first as a rock fall and a rotational slide involving the rocks of the Autapie–Pelat nappes between 1900 and 1600 m of altitude, just under the "Rocher Blanc". This process triggered the destabilisation of the "Terres Noires" and moraines, and the progressive advance of the clays and marls terrains in the gorge of the La Valette stream, cut in the "Terres Noires". A geophysical study made by Evin (1992) by means of seismic profiles in the middle part of the landslide estimates a depth of about 25 m of the sliding surface. Two main events occurred in spring 1989 and in autumn 1992 with velocity peaks of 50 cm/day. Apart from them,

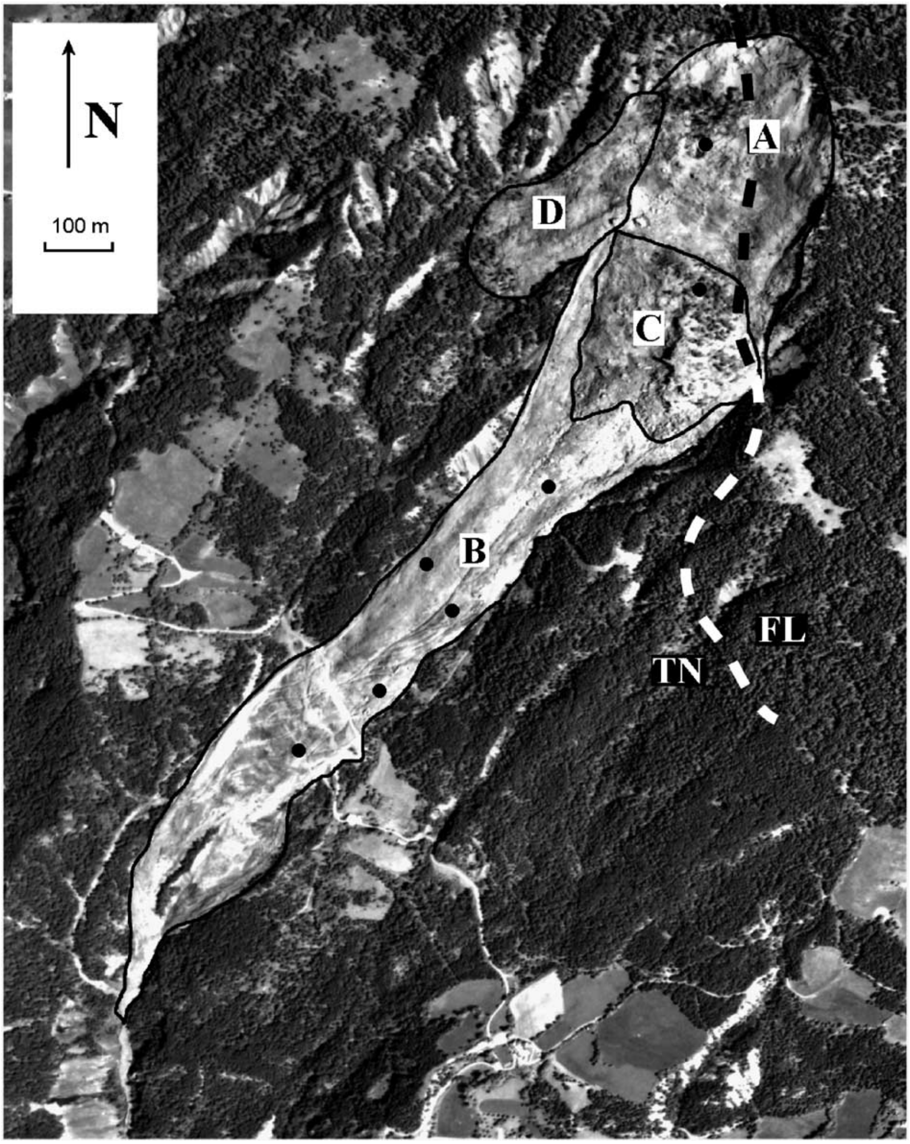

Fig. 2. Aerial photograph of the La Valette landslide taken in May 1996. The dashed line represents the tectonic contact between the "Terres Noires" formation (TN) and the Helminthoid Flysch (FL). A, B, C, D are the four zones identified on the basis of geological and geomorphological study and described in the text. The black points represent the location of the ground laser measurements on the landslide. The reference point is placed on the facing slope.

the motion is quite uniform, with some seasonal variations and maximum displacements amounting to 10 cm/day. The instability involves now the slope from 1900 m of altitude down to 1300 m, with a length of about 2000 m and a width of 450 m at the top of the landslide.

The landslide motion has been constantly monitored by "Restauration des Terrains en Montagne" Service (RTM) since 1988 by means of laser geodetic ground measurements made every 3 weeks on a section located in the middle part of the landslide and, since 1993, at around 20 points located inside and outside the landslide. Fig. 2 presents the monitored points, whose displacement values have been used in the present work for comparison with the motion values derived from the interferometric study.

4. Aerial photograph interpretation

From the analysis of the landslide by means of ground surveys and aerial photograph interpretations, four zones have been distinguished and mapped; they are characterized by different geometric and geomorphological features (Fig. 2). The upper part (zone A in Fig. 2) includes a nearly vertical scarp formed in the black schists of the Autapie nappe, corresponding to the crown of the initial rotational slide reshaped by the subsequent landslide evolution. At the base of this scarp, a rocky outcrop (the limestone scales of the Pelat nappe), about 200 m wide in E–W direction ("Rocher Blanc"), produces a local decrease in the steepness of the slope, highlighted by thin trees on the aerial photograph (Fig. 2). The geometry of fractures present in the limestone leads to the development of a steep rocky escarpment, from which abundant rock falls occur, producing a steep debris accumulation of rock masses up to some cubic meters in volume (zone C in Fig. 2). In the lower part (sector B in Fig. 2), the instability phenomenon develops as an earth-flow, characterized by a more regular morphology and by some 1–2 m-deep gullies caused by the surface water erosion along the preexisting fractures. The earth-flow seems to show a non homogeneous displacement field. As testified also by the distribution of the vegetation, two kinematically different sectors apparently exist, separated by the country road. Starting from the sector A (Fig. 2), a second earth-flow has developed and still develops with the same characteristic of the main body of the landslide (sector D in Fig. 2). The terminal part of the sector B earth-flow is susceptible to transform in a mud-flow following long and high-intensity precipitations.

5. Data set for the motion analysis

Thirty SAR images acquired by the European remote sensing satellites ERS-1 and ERS-2 between 1991 and 1999 have been used. Because of the specific geographical orientation of the investigated slope, facing S–SW, only images acquired in descending orbits have been processed. Furthermore, due to the relatively fast landslide motion (between 1 and 3 cm/day over the studied period), radar images with short temporal interval have been chosen. These images have been acquired in the TANDEM phase (1-day time interval) and in the ERS Commissioning phase (3-day passes). From those images, 15 interferograms exhibiting significant coherence in the landslide slope have been retained (Fig. 3). The differential interferograms were produced with the technique of

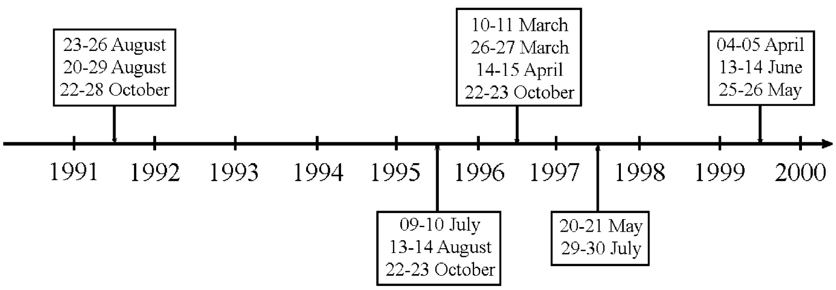

Fig. 3. SAR interferometric pairs processed in the present work. Except for the 1991 data, the interferograms are based on TANDEM pairs.

the two-pass differential interferometry with Digital Elevation Model (DEM) subtraction (Massonet et al., 1993), using a 15 m accuracy DEM provided by the National Geographical Institute of France (IGN). The interferograms have been processed and geocoded with a 10×10 m pixel resolution. Because the direction of the average landslide slope is nearly parallel to the line of sight of the satellite, the component of displacement inferred from the interferograms is near the real displacement along the slope. As on each interferogram the phase variation is less than 2π, no phase unwrapping has been attempted.

6. One-day motion detected by interferometric analysis

In a first step, we focus the analysis on the 22–23 October 1995 TANDEM differential interferogram (Fig. 4). This differential interferogram exhibits significant phase variations associated with the landslide.

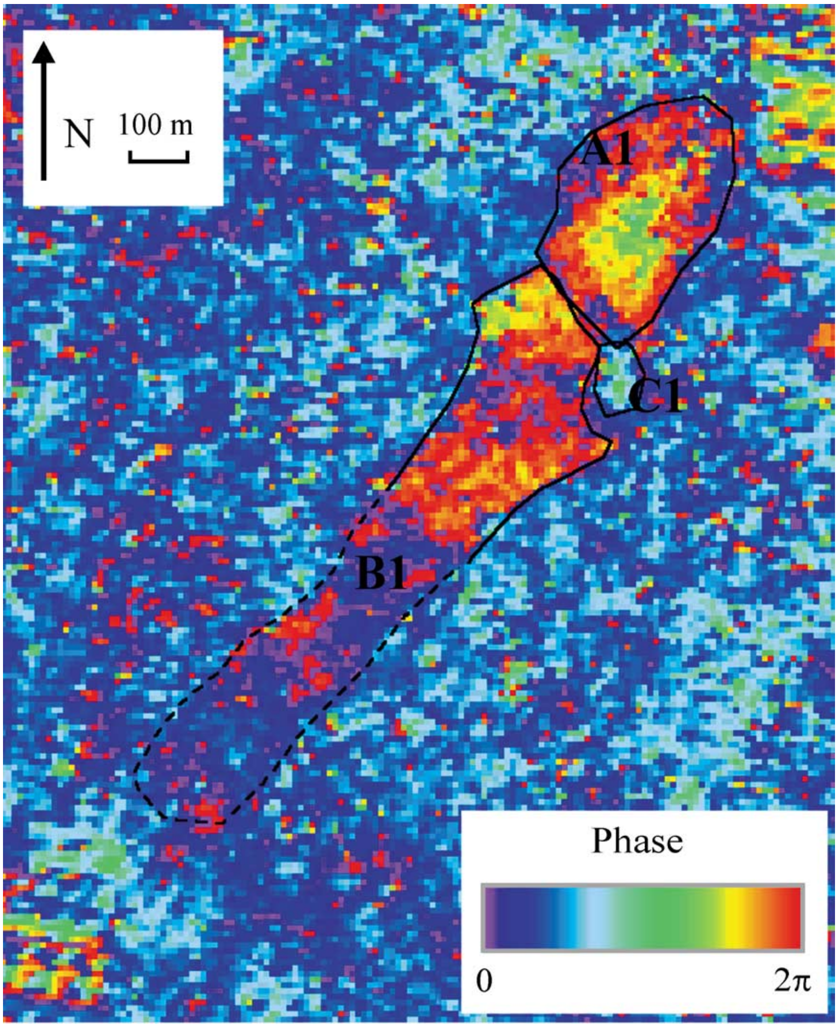

Fig. 4. One-day geocoded differential SAR interferogram dated 22–23 October 1995 representing the surface displacement along the line of sight (see text for explanations). Three areas distinguished from SAR interferometric analysis on the basis of the fringe shape variations are shown (A1, B1, C1). Phase variation of 2π corresponds to a displacement of 2.8 cm.

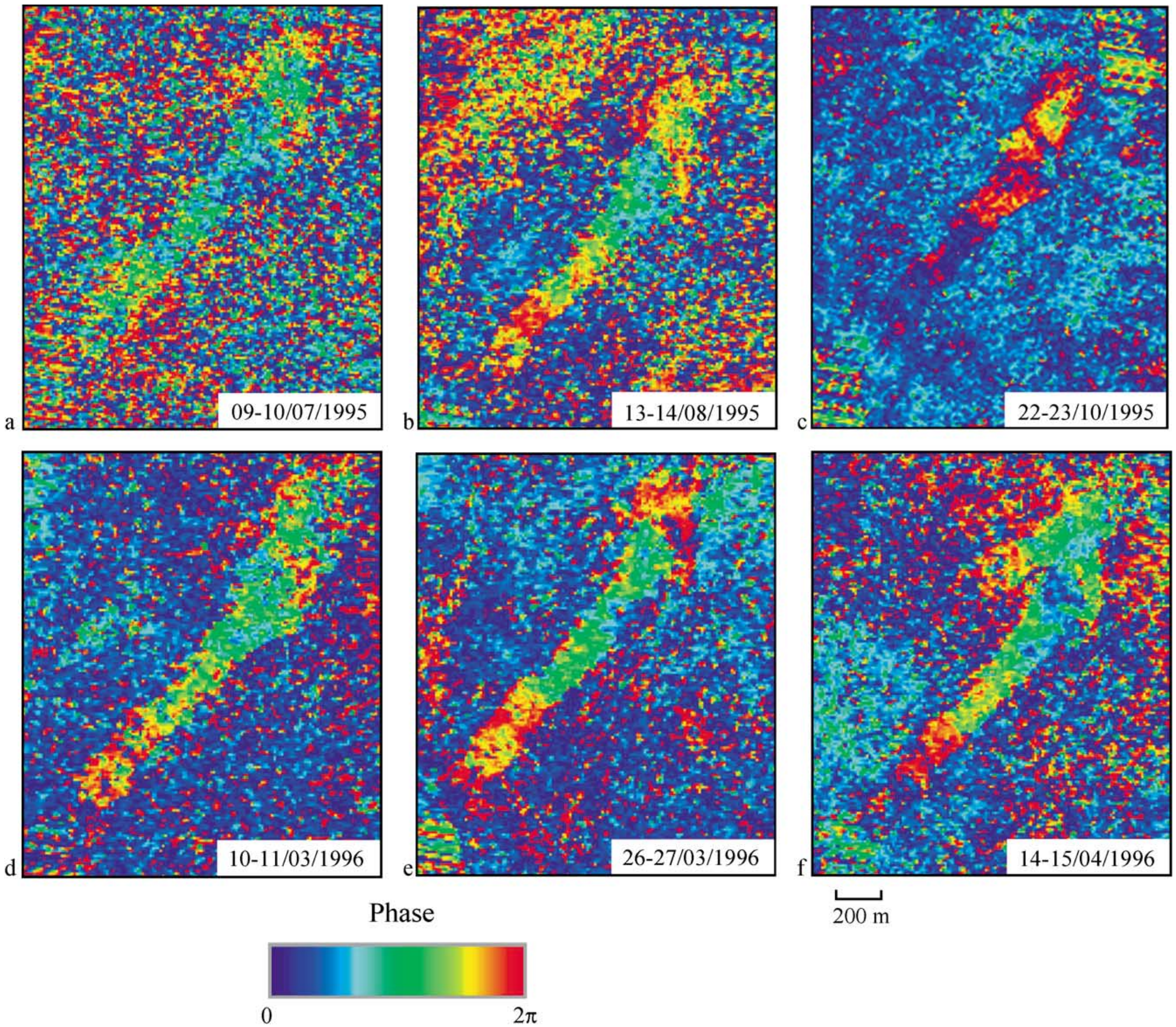

Fig. 5. Multitemporal interferometric series from July 1995 to April 1996.

Indeed, the boundary of the motion area can be mapped. Three areas can be isolated based on the variation in the fringe characteristics.

The zone A1 (Fig. 4) in the upper part of the landslide is characterised by a rounded shape of the fringes. As a full-phase rotation corresponds to a displacement of 2.8 cm, the maximum displacement in this area is 1.7 cm. The upper part of the zone A1 is limited by the crown and the main scarp of the landslide; the nearly linear lower limit coincides with the "Rocher Blanc" outcrop. The phase variation indicates that the landslide develops with a rotational mechanism in this area, in agreement with the precedent in situ observations (Potherat, 2000).

The lower part (zone B1 in Fig. 4) corresponds to the main body of the landslide, where the displacements reach a maximum value of 1.1 cm and seems to be uniform. In this part, the landslide movement is mainly translational, in a direction parallel to the slope.

Finally, a small area of around 100×100 m is observed in the eastern part (zone C1 in Fig. 4); it appears to be affected by a smaller displacement as compared to the rest of the landslide. This isolated area could be related to the displacement of the 'Rocher Blanc', which is a resistant rocky outcrop present in the landslide.

The three areas mapped from SAR interferometry (A1, B1, C1 in Fig. 4) correspond in part to the areas A, B, C (cf. Fig. 2) defined on the basis of ground observations and aerial photograph interpretation. Some discrepancies regarding the boundaries and the dimensions of the three areas (e.g., C1 is smaller than C) may indicate that the morphology is not always directly related to the landslide motion. Furthermore, the eastern part of the landslide (zone D in Fig. 2) is not distinguished on the interferogram. This can suggest that the deformation rate of this sector is under the detection threshold of SAR interferometry (Delacourt, 1997) or the presence of nonstationary deformations.

7. Seasonal motion variations on 1995–1996 interferograms

After the analysis of motion features on one interferogram, the temporal variation of the landslide activity over 1 year has been studied, using six TANDEM differential interferograms with images acquired between July 1995 and April 1996. (Fig. 5). The six differential interferograms exhibit significant phase variations and this confirms the landslide activity.

The three areas defined on the 22–23 October interferogram can still be distinguished. Furthermore, on the interferograms in Fig. 5a, d and f, corresponding to July 1995, March and April 1996, respectively, it is possible to recognize a lobate-shaped sector developing on the northwestern side of the landslide scarp. This area corresponds to the zone D shown in Fig. 2. The evolution of this small sector seems to be quite independent from the main body of the landslide. It is affected by a nonstationary motion and

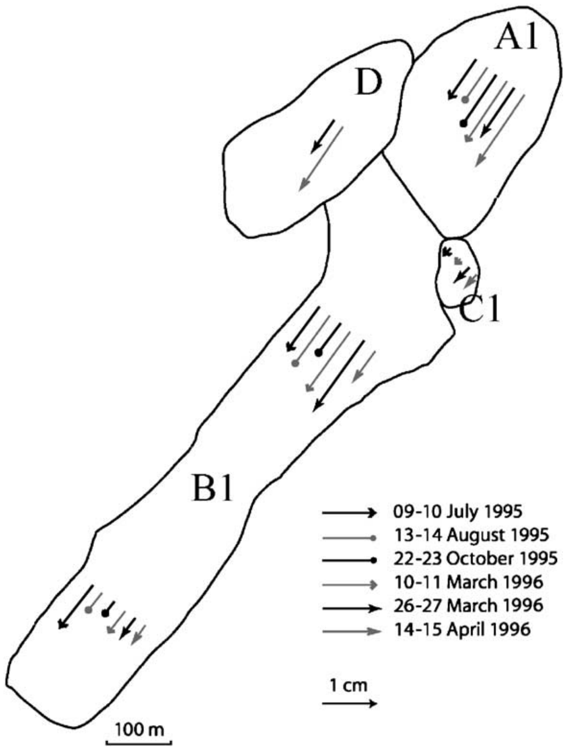

Fig. 6. Displacement vectors for the 1995–1996 data set for each of the four mapped landslide zones. The vector set represents the maximum displacements registered. For the B1 zone, two vector sets are presented: the upper one represents the maximum displacement values for the B1 zone; the lower one corresponds to the value of the lower part of the area. This shows the temporal and spatial heterogeneities of the landslide motion.

probably by an acceleration in spring and summer times. In fact, only in this period the amount of displacement of the sector D is comparable with that of the main body of the landslide composed by sectors A1 and B1 (Fig. 6).

The nonstationarity of the rate of deformation of the sector D of the landslide can be due to different groundwater conditions in comparison with the main body of the landslide. A hydrogeological study of the landslide slope (Dupont and Taluy, 2000) shows that most of the springs present in the landslide gushes out in the eastern side. This water is drained away through surface channels constructed by the RTM Service in an attempt to stabilize the landslide. On the contrary, no drainage system was realised in the western part of the slide (zone D). Therefore, this part is maybe more sensible to groundwater variations. In addition, a smaller volume of material is involved in this second earth-flow.

Moreover, the movements of the upper zone (A1) are not always correlated with the movements of the lower one (B1) (Fig. 6), probably because of the different mechanisms controlling the motion rotational and translational, respectively. Nevertheless, the maximum displacement rates reached in both sectors on the days corresponding to the interferograms studied are the same (i.e., around 2 cm/day). Furthermore, within the sector B itself, some nonuniform deformations occur, with the lowest velocities present at the toe of the landslide. The sector C in the eastern part of the landslide is affected by a slower motion (< 1 cm/day). This is consistent with the structure of the "Rocher Blanc".

No evidence of correlation between seasonal meteorological data and variation in the rate of landslide deformations has been observed. This landslide behaviour has already been pointed out by Flageollet et al. (1999) on the basis of long-term observations.

A comparison of the displacement values deduced from SAR interferograms analysis with the laser geodetic measurements made by RTM Service on some points placed in the landslide slope (Fig. 2) has also been carried out. The ground data collection is not regular; in some cases, a few months can pass between two acquisitions. Over the radar acquisition periods, the temporal ground data sampling is of 1 month. In order to facilitate the comparison with the 1-day motion interferometric values, stationary motion between two ground-based measurement acquisition has been assumed. A correlation between the results obtained from the two methods of investigation is shown in Fig. 7. Even if the dates of data acquisition by each method

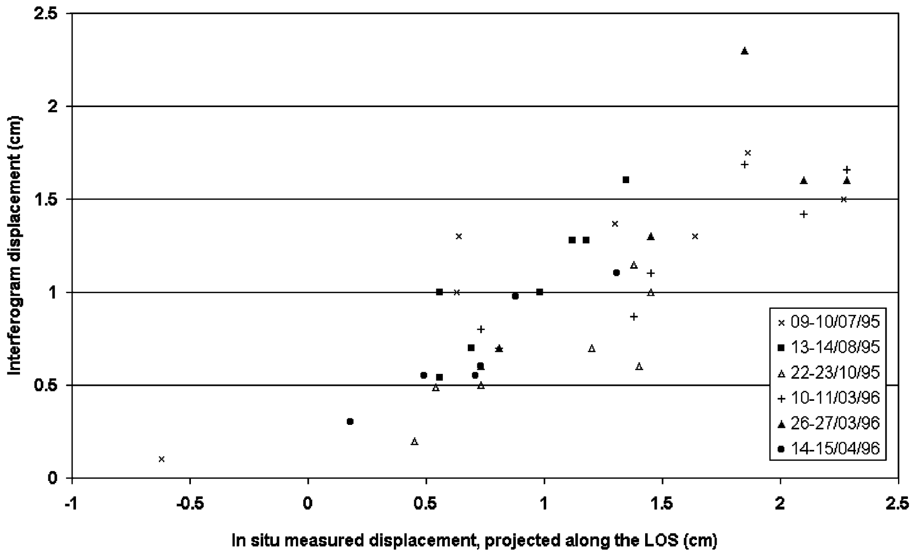

Fig. 7. Comparison between the ground displacement measurements projected along the line of sight of the satellite (x-axis) and the SAR interferometric displacement values (y-axis) for the 1995–1996 interferometric set. The average correlation coefficient is 0.88.

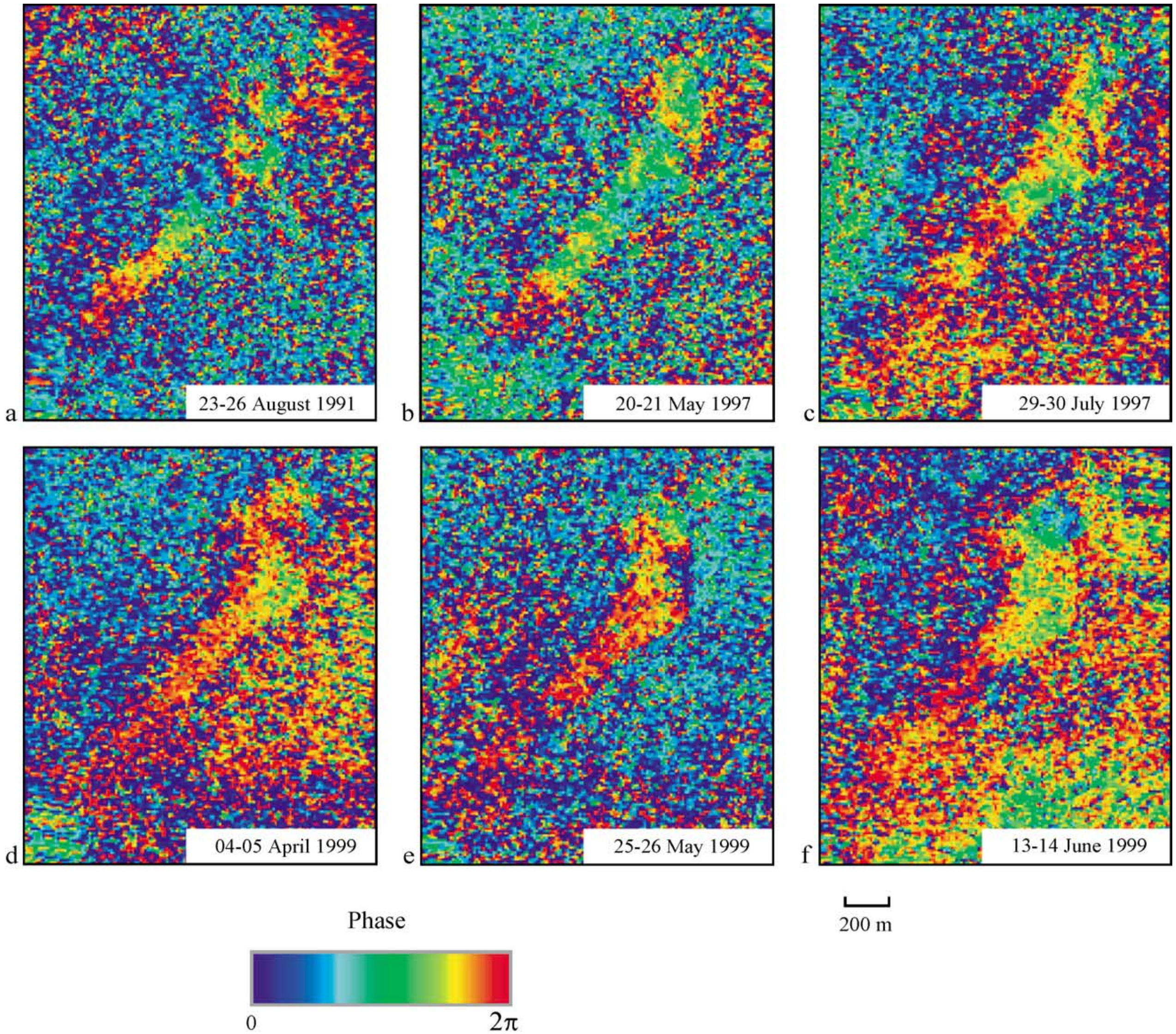

Fig. 8. 1991 – 1997 – 1999 geocoded differential interferograms.

are different, the correlation is high. This indicates that the velocities obtained on 1-day interferograms are globally stationary over periods of 1 month, which is the frequency of ground measurements.

In conclusion, the multitemporal analysis of the six interferograms from July 1995 to April 1996 shows that the landslide motion has not been stationary, varying in the time on one year scale and in the space over the whole landslide. The reasons of this variability are not clearly understood, but could be influenced by the local differences in the hydrogeological conditions. The differences in the deformation rates between the observed areas of the landslide suggest that three sectors A, B and D (previously defined) are influenced by three different and independent landslide mechanisms.

8. Nine-year variation of the landslide motion

The general evolution of the landslide motion over 9 years has been studied by means of some interferometric tandems dating 1991, 1995, 1996, 1997 and 1999. Fig. 8 shows six new differential interferograms, from which landslide motion can be inferred. The 1991 SAR images were acquired during the ERS commissioning phase (3 days apart). Change in the vegetation state and the increased amount of deformation due to the longer time span with respect to the 1-day interferograms lead to a decrease of coherence. Therefore, both deformation rates and boundaries of moving areas are more difficult to estimate (Fig. 8a). The two interferograms dated 1997 show a gradient of deformation lower than in 1995–1996; this is also in agreement with the RTM Service ground data measurements. The shape of the landslide is clearly detectable in Fig. 8b, while in Fig. 8c, the lower part of the landslide is not easily distinguished from the noise, probably due to the slow motion. The lowering of the landslide velocity continues in 1999; in the related interferograms (Fig. 8d, e and f), the upper part of the landslide is always detectable, even if the signal-to-noise ratio has decreased. The landslide boundaries on the lower part become gradually blurred, and this suggests the decreasing motion rates approach the detecties limit of the method.

The average daily velocity of the landslide (Fig. 9), calculated as mean value of the two zones characterized by high coherence, one in the upper and one in the lower part, is of 1 cm/day in 1991 and increases to 2 cm/day during 1996. Then, the velocity in the upper part decreases to about 0.4 cm/day in 1999.

Furthermore, using the results of the interferometric analysis, an attempt has been made to map the boundaries of the effective motion zones of the

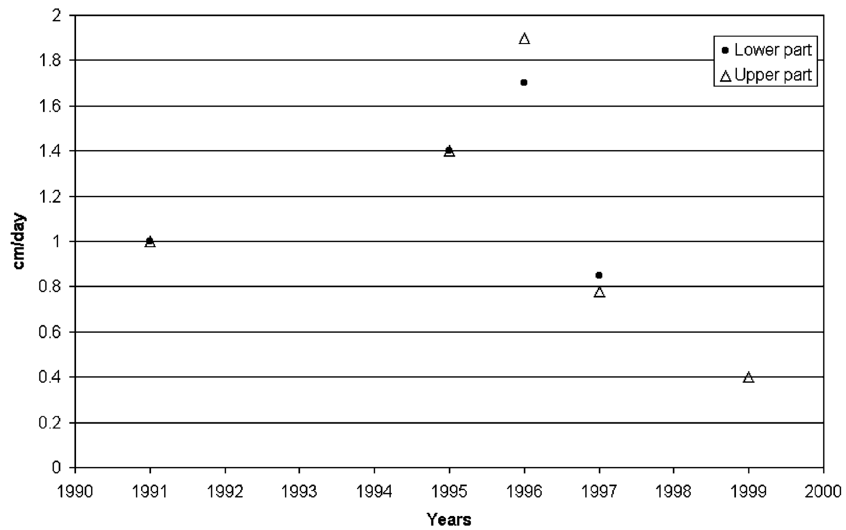

Fig. 9. Variations in the average daily velocity of the landslide between 1991 and 1999 deduced from interferometric study.

landslide (Fig. 10). Despite the low coherence of the 1991 interferometric products, it seems that the moving zones have enlarged both in the upper and in the lower part from 1991 to 1995–1996, respectively, due to a retrogression of the main scarp and downslope progressive movements of the main body of the landslide. The 1997 and 1999 interferograms were not used in this case because of the lower landslide velocities. Indeed, in the slowest part of the landslide, the ground surface changes are under the detectability threshold of SAR interferometric technique.

9. Discussion and conclusions

Despite severe limitations, such as specific constrains on the orientation of the landslide, loss of coherence due to change of ground surface state, atmospheric artefacts, monodirectional value of the

Fig. 10. Changes in the landslide boundaries between 1991 and 1996 deduced from SAR interferometry analysis marked on the aerial photograph.

displacement and dependence on the orbit cycle, under favourable conditions, the differential SAR Interferometry is a potentially useful technique to investigate landslides with displacement rates below a few centimeter per day. The present application of the SAR Interferometry technique on the La Valette landslide confirms the first results obtained on the same site by Vietmeier et al. (1999), such as the validation of the displacement values deduced from the interferogram analysis with the ground measurement data and the change of activity of the landslide between successive SAR image acquisitions. Moreover, the use of the DEM elimination technique allows for a more accurate subtraction of the topographic data, leading to a better estimation of the displacement values.

In this study, this technique has been applied to extend temporally the previous analysis (Vietmeier et al., 1999) of the landslide to 9 years. The average daily landslide velocities deduced by interferometric product analysis are in accordance with the ground observations made by RTM Service. They amount to 1 cm/day in 1991, increase to 2 cm/day during 1996 and decrease to 0.4 cm/day in 1999. Some difficulties in the interferometric product interpretation have been encountered, especially in the case of 1999 interferograms, in which the landslide displacement was smaller and the landslide boundaries less detectable than in the other interferograms. Moreover, the presence of some atmospheric artefacts was inferred in the eastern sector of the 1999 interferograms (Fig. 8d and f), where a phase variation unrelated to landslide movement complicated the interpretation.

On a 1-year scale, six ERS-1 and ERS-2 TANDEM interferograms revealed considerable spatial and temporal variability of the landslide movements, probably related to the different hydrogeological conditions. However, a correlation between this variability and meteorological events was not possible because of the insufficient quantity of SAR data over the whole year. Finally, an integrated aerial photograph interpretation and geomorphological analysis was used. Four domains with characteristic velocity fields and characteristic morphologies were detected. The landslide enlargements were observed both in the upper and in the lower part, respectively; these were caused by a headscarp erosion and a downslope progression of the main body of the landslide.

Acknowledgements

This work has been financially supported by ACI-'Prévention des catastrophes naturelles', PNRN and PNTS French INSU program. SAR Images have been provided by ESA. Lasermeter measurements have been supplied by RTM Service. We would like to warmly thank G. Warowski for his editor work.

References

Antoine, P., Giraud, A., Meunier, M., Van Asch, T., 1995. Geological and geotechnical properties of the "Terres Noires" in south–eastern France: weathering, erosion, solid transport and instability. Eng. Geol. 40, 223–234.

Carnec, C., Massonet, D., King, C., 1996. Two examples of the use of SAR interferometry on displacement fields of small spatial extent. Geophys. Res. Lett. 23 (24), 3579–3582.

Colat, G., Locat, J., 1993. Glissement et coulée de La Valette dans les Alpes de Haute–Provence. Présentation générale et modélisation de la coulée. Bull. Liaison - Presse etud. Ch. 187, 19–28.

Delacourt, C., 1997. Détection et analyse de mouvements de surface par interférométrie différentielle, PHD, IPGP, 199 pp.

Dupont, M., Taluy, P., 2000. Hydrogélogie du glissement de la Valette (avec carte au 1/5000ème des venues d'eau). Rapport du D.E.A., Université de Savoie.

Evin, M., 1992. Prospection sismique en partie basse. RTM Report.

Flageollet, J.C., Maquaire, O., Marin, B., Weber, D., 1999. Landslides and climatic conditions in the Barcelonette and Vars basins (Southern French Alps, France). Geomorphology 30, 65–78.

Fruneau, B., Achache, J., Delacourt, C., 1996. Observation and modelling of the Sant-Étienne-de-Tinée landslide using SAR interferometry. Tectonophysics 265, 181–190.

Fruneau, B., Rudant, J.P., Obert, D., Raymond, D., 1999. Small displacements detected by SAR Interferometry in the city of Paris (France). Proc. IGARSS '99, Hamburg, Germany, 28 June–2 July, 1943–1945.

Goldstein, R.M., Englehardt, H., Kamb, B., Frolich, R.M., 1993. Satellite radar interferometry for monitoring ice sheet motion: application to an Antarctic Ice Stream. Science 262 (1), 525–530.

Kerckhove, C., 1969. La "zone du Flysch" dans les nappes de l'Embrunais (Alpes Occidentales). Géol, Alpine 45, 5–204.

Kerckhove, C., Debelmas, J., Cochonat, P., 1978. Tectonique du soubassement parautochtone des nappes de l'Embrunais–Ubaye sur leur bordure occidentale, du Drac au Verdon. Géol. Alp. 54, 67–82.

Massonet, D., Rossi, M., Carmona, C., Adragna, F., Peltzer, G., Feigl, K., Rabaute, T., 1993. The displacement field of the Landers earthquake mapped by radar interferometry. Nature 364, 138–142.

Massonet, D., Briole, P., Arnaud, A., 1995. Deflation of Mount Etna monitored by spaceborn radar interferometry. Nature 375, 567–570.

Potherat, P., 2000. Projet de recherches sur le thème: Risques naturels et prévention, Contribution LCPC.
Rott, H., Scheuchl, B., Siegel, A., Grasemann, B., 1999. Monitoring very slow slope motion by means of SAR interferometry: a case study from a mass waste above a reservoir in the Ötztal Alps, Austria. Geophys. Res. Lett. 26 (11), 1629–1632.
Vanderbecq, A., 2000. Potentiel de l'interférométrie en zones montagneuses. DEA Dynamique de la Lithosphère, Grenoble. 78 pp.
Vietmeier, J., Wagner, W., Dikau, R., 1999. Monitoring moderate slope movements (landslides) in the southern French Alps using differential SAR interferometry. Proc. Fringe.
Zebker, H.A., Rosen, P., Goldstein, R.M., Gabriel, A., Werner, C.L., 1994. On the derivation of coseismic fields using differential radar interferometry: the landers earthquake. J. Geophys. Res. 99 (B10), 19617–19634.